

Synthesis of Dye-sensitized Solar Cell Using Nickel-tetraphenylporphrine as a Sensitizer

¹FAWAD AHMED, ¹MUHAMMAD ATHAR ABBASI*, ¹AZIZ-UR-REHMAN,
¹MUHAMMAD ASLAM AWAN, ²MUHAMMAD ASIF IQBAL, ³SYEDA AMBAR YOUSAF,
²MUHAMMAD JAVED IQBAL AND ⁴VIQAR UDDIN AHMAD

¹Department of Chemistry, Government College University, Lahore-54000, Pakistan.

²Department of Chemistry, Government College of Science, Wahdat Road, Lahore, Pakistan.

³Department of Physics, Government College University, Lahore-54000, Pakistan.

⁴HEJ Research Institute of Chemistry, International Center for Chemical and Biological Sciences, University of Karachi, Karachi-75270, Pakistan.

(Received on 9th February 2010, accepted in revised form 10th March 2010)

Summary: A dye-sensitized solar cell was prepared under facile conditions. For this, a wide range of metalloporphyrines was investigated and consequently Ni-tetraphenylporphrine was selected because it gave the maximum output in terms of voltage, current, and power. The structures of the prepared dyes were determined by single crystal X-ray diffraction (SCXRD) method. The molar extinction coefficient (ϵ) of Ni-tetraphenylporphrine in chloroform was determined ($3.36 \times 10^5 \text{ dm}^3 \text{ cm}^{-1} \text{ mol}^{-1}$ at 413 nm). Glass electrode was made using dip-coating technique, which had resistivity of 12.5 Ωcm coated with fluorine doped tin oxide (FTO) layer. It was analyzed by checking its transparency and electrical conductivity. Its compositional analysis and structural determination was carried out by X-ray powder diffraction (XRD). The analysis showed the crystalline structure of SnO_2 . Grain size calculations depicted the particle size of order of 2-5 nm. Scanning Electron Microscope (SEM) revealed the nanocrystals of SnO_2 . Its band gap was (3.8 eV). The UV-Visible spectrum showed high transparency of glass electrode. Thickness of the film (SnO_2) was calculated by surface profilometry, and thickness obtained about 100 nm. Photoelectrochemical measurements indicated that the cell present short-circuit photocurrent (J_{sc}) of 90 A/m^2 , fill factor (FF = 0.37), photovoltage ($V_{oc} = 0.60 \text{ V}$), and overall conversion efficiency (η) of 2 % under standard test conditions (STC).

Introduction

Dye-sensitized solar cells (DSCs), which convert light to electricity by means of harvesting of solar radiation by the sensitizers, have attracted considerable attention in scientific research and for practical applications. The intrinsic advantages of these devices are high photoelectrical efficiency over a large span of the visible light spectrum under direct sunlight and diffuse light conditions. Moreover, it has low cost compared to the traditional solid-state crystalline silicon solar cells. Most of the dye-sensitized solar cells are made from nanoporous TiO_2 photoelectrodes sensitized with ruthenium (II) complexes [1]. The investigation and development of the dye-semiconductor systems are essential for long-term applications of dye-sensitized solar cells. SnO_2 is a stable, n-type, wide band-gap semiconductor ($E_g = 3.6 \text{ eV}$) that has been used for various applications, including solid-state gas sensor, photovoltaic devices, dye-based solar cells, transparent conductive films for display and solar cells, catalysis, and anode

materials of secondary lithium ion battery [2-6]. Although SnO_2 is a better electron acceptor since its conduction band edge lies $\sim 0.5 \text{ V}$ more positive than that of TiO_2 [7], but the investigations concerning dye-sensitized solar cells based on SnO_2 nanoporous photoanodes are still far from perfection [8].

Several methods were used for deposition of the films, which include chemical vapour deposition (CVD), sputtering, thermal evaporation, pyrosol, and sol-gel-dip-coating technique (SGDC). SGDC method has a several advantages over the other methods such as, it is a low-cost, and simple process, precise control over doping level is easier, possibility of using high purity starting materials and coating of large, and complex shaped substrates is also easier [9]. In order to improve the photovoltaic performance, and stability of DSCs, extensive efforts have been focused on the search of new highly efficient sensitizers. Recent studies have been

*To whom all correspondence should be addressed.

emphasized that sensitizers with high molar extinction coefficients are effective means of augmenting the efficiency of dye-sensitized solar cells [1]. The metalloporphyrins are the derivative of the synthetic porphyrins, and naturally occurring porphyrins were previously employed as sensitizers [10]. In the present study, we investigated the use of SnO₂ nanoporous to be used as photoanode in a dye-sensitized solar cell. The nanoporous oxide was prepared by dip-coating technique as reported earlier [9], but with slight modifications to get better results. To the best of our knowledge, no dye-sensitized solar cell with Ni-tetraphenylporphyrine as a sensitizer and ZnO as semiconductor layer has been reported so far. The photoelectrochemical properties of Ni-tetraphenyl-porphyrine dye-sensitized SnO₂ electrode were carried out by current-voltage measurements.

Results, and Discussion

Characterization of SnO₂ Film

XRD patterns of prepared SnO₂ by dip-coating are shown in Fig. 1a. The diffraction peaks from the SnO₂ at $2\theta = (26.48^\circ, (33.74^\circ, (37.80^\circ, (51.56^\circ, (54.53^\circ, (64.45^\circ, (70.95^\circ, \text{ and } (78.35^\circ)$ to the (110), (101), (200), (211), (220), (112), (202), and (321) diffraction planes, respectively. These diffraction planes can be indexed to the tetragonal rutile structure of SnO₂ [3]. No obvious reflection peaks from impurities, such as unreacted Sn or other than tin oxides were detected, indicating the high purity of the product.

In (Fig. 1a) XRD pattern was not close to the standard SnO₂ XRD pattern, probably due to the use of ethyleneglycol solvent because it is not easily evaporated, and deposition of the film may not be uniform. But in case of (Fig. 1b) when small proportion of methanol was added the volatility of the solution increased, and hence the uniformity and

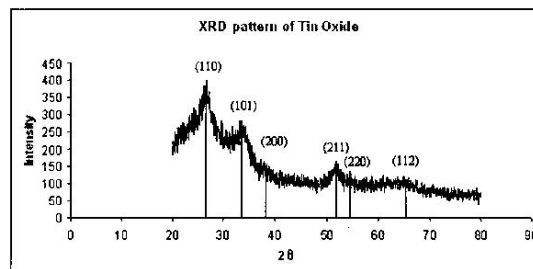


Fig. 1a: XRD pattern of SnO₂ when solvent was ethyleneglycol.

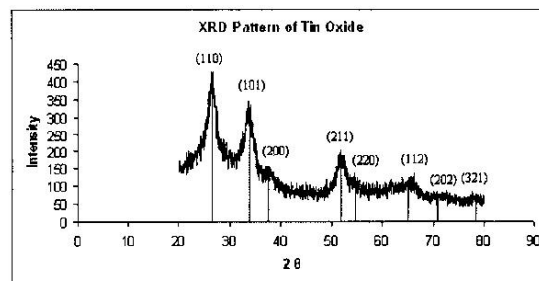


Fig. 1b: XRD pattern of SnO₂ when solvent was mixture of ethyleneglycol, and methanol in ratio (7:3) for deposition on glass substrate.

exact crystallinity of SnO₂ was obtained. The determined average size (Estimated Crystallite Size) of the prepared SnO₂ tetragonal rutile crystallite was 2-5 nm.

Scanning Electron Microscopy (SEM) was employed to perform the surface characterization of the deposited film. The SEM images, presented in Fig. 2a showed that the film exhibited an almost flat and well-distributed network of surface features. It was noted that the particles having certain homogeneity in size, and nearly spherical shape. The top view of the porous SnO₂ film was also examined

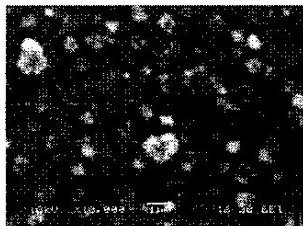


Fig.2a: Low resolution SEM images of SnO₂ film.

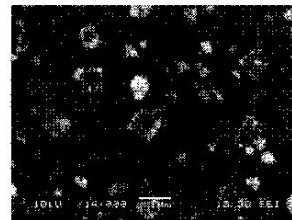


Fig.2b High Resolution SEM images of SnO₂ film.

using a lower magnification (high magnification) to show the progress of formation of SnO₂ layer (Fig. 2b).

UV-visible absorption spectrum was carried out in order to characterize the optical absorbance of the SnO₂ thin film. It is well known that the absorption coefficient of an amorphous semiconductor has a characteristic relation [5].

$$(\alpha h\nu)^2 = A(h\nu - E_g)^{n/2}$$

where α is the absorption coefficient, A is a constant, E_g is the band gap, and n equal to one for direct allowed transition. Therefore, the band gap can be estimated from a plot of $(\alpha h\nu)^2$ versus photon energy ($h\nu$). The intercept of the tangent to the plot will give a good approximation of the band gap energy for this direct band gap material, (Fig. 3).

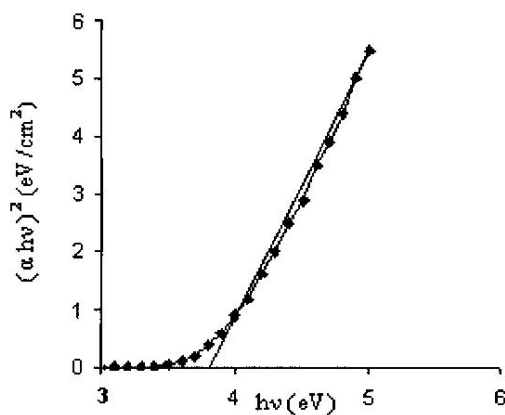


Fig. 3: Energy band gap plot.

Optical transmittance of FTO film deposited on glass substrate

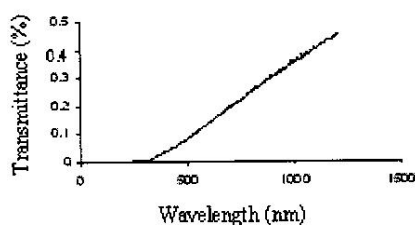


Fig. 4a: Transmission of SnO₂ when solvent was mixture of ethyleneglycol, and methanol in ratio (7:3) for deposition on glass substrate.

Optical transmittance of FTO film deposited on glass substrate

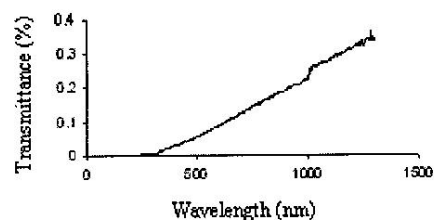


Fig. 4b: Transmission of SnO₂ when solvent was only ethyleneglycol for deposition on glass substrate.

The band gap energy of the as-prepared SnO₂ thin film was calculated, and found to be 3.8 eV, which is higher than that of the reported SnO₂ [5,9].

It was noted that when the solvent was the mixture of ethyleneglycol, and methanol better transmission, and transparency of FTOs (Fig. 4a) was obtained as compared to that with ethyleneglycol FTOs only (Fig. 4b).

Ellipsometric Analysis of SnO₂ Film on Glass Substrate

The Photocurrent-voltage characteristics of prepared solar cell under direct sunlight irradiation was measured, and shown graphically in Fig. 5a. The current voltage characteristics of FTO film revealed the ohmic behavior at room temperature as shown graphically in (Fig. 5b).

Characterization of Dye

Single crystal X-ray diffraction of metalloporphyrines, and porphyrine was done, and the obtained data matched closely with the reported one [11] proving the structure of the dyes as shown in (Fig. 6a, and b), respectively.

The unit-cell parameters of Ni-TPP, and tetraphenylporphyrine (TPP) are listed in Tables-1, and 2, respectively.

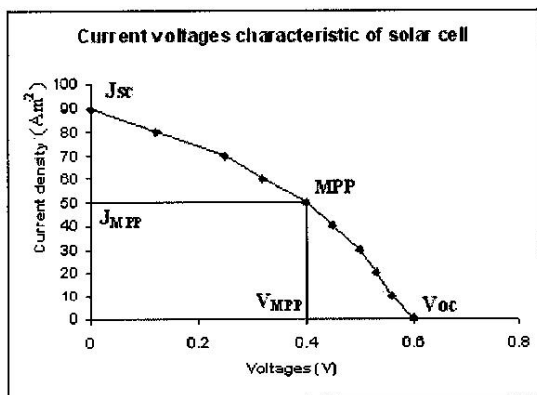
Table-1: Unit-cell parameters of Ni-TPP.

Cell Structure Tetragonal

a	b	c	α	β	γ	R(int)	R(sigma)
15.1045	15.1045	13.8946	90	90	90	0.051	0.0558

Table-2: Unit-cell parameters of Tetraphenylporphrine (TPP).

Cell Structure Triclinic							
a	b	c	α	β	γ	R(int)	R(sigma)
6.4331	10.4617	12.3948	95.857	99.265	101.221	0.0605	0.0825

Fig. 5a: Photocurrent-voltage characteristics of dye sensitized solar cell device based on Ni-TPP sensitized, SnO₂ electrode.

Current-voltage characteristics of FTO film

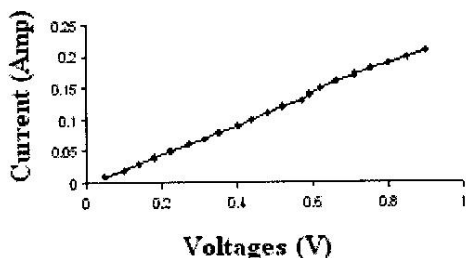


Fig. 5b: Current-voltage characteristics of FTO films.

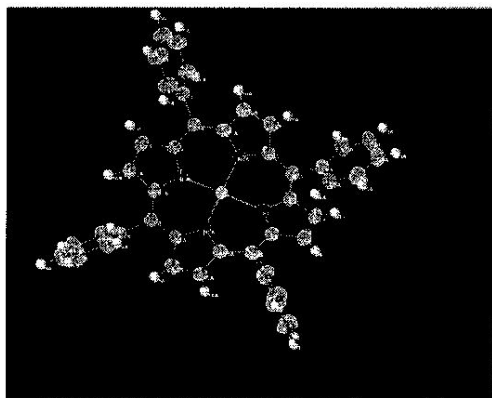


Fig. 6a: Single crystal X-ray structure of Ni-TPP.

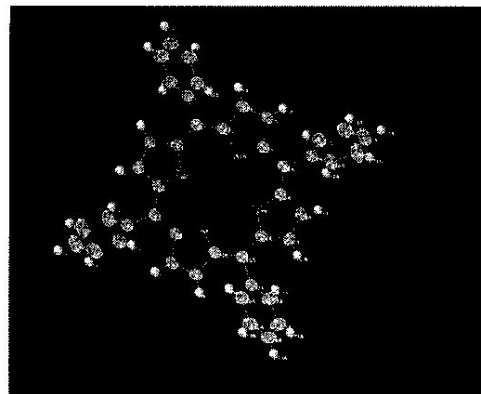


Fig.6b: Single crystal X-ray structure of TPP. (Tetraphenylporphrine)

Spectral Characteristics of Ni-tetraphenylporphrine

The (Fig. 7) shows UV-Visible absorption spectrum for Ni-tetraphenylporphrine in chloroform solution. Ni-tetraphenylporphrine exhibited two π - π^* electron-transition peaks (413, and 442 nm) in the visible region. The 413 nm peak showed a broad feature contributing broadly to the light-harvesting (LHF) efficiency. The molar extinction coefficient (ϵ) of Ni-tetraphenylporphrine in chloroform was determined to be ($3.3 \times 10^5 \text{ dm}^3 \text{ cm}^{-1} \text{ mol}^{-1}$ at 413 nm), which is about twenty two times larger than that of ruthenium polypyridyl complexes ($1.42 \times 10^4 \text{ dm}^3 \text{ cm}^{-1} \text{ mol}^{-1}$ at 532 nm) [12]. Because of the high extinction coefficient, and broad visible-light absorption of Ni-tetraphenylporphrine, it is feasible to produce solar cells with high efficiency. We have fabricated a glass SnO₂ based cell as: Glass/SnO₂-dye//electrolyte//Al/Glass.

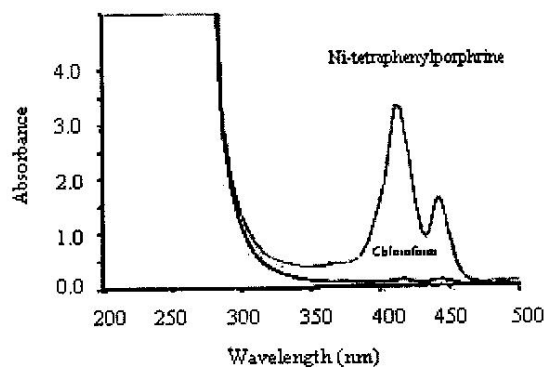


Fig 7: The UV-vis absorption spectrum for Ni-TPP (tetraphenylporphrine) in chloroform.

Experimental

Chemicals and Solvents

All the chemicals, and solvents involved in the study were obtained from Merck (Pvt.) Ltd. (Germany).

Preparation of Metalloporphyrines (Ni-tetraphenylporphyrine)

Various metalloporphyrines were taken under consideration, and finally Ni-TPP (nickel-tetraphenylporphyrine) was prepared by a slight modification in the reported method [13] to get improved results.

Tetraphenylporphyrine (TPP) was prepared by the reaction of (8.31 mL) benzaldehyde, and (5.81 mL) pyrrol. The reaction mixture was refluxed in the presence of propionic acid (312.5 mL) for about 45 minutes at 141 °C, and cooled, and kept for two days. After two days, sharp bright violet crystals of TPP were formed. The obtained crystals were recrystallized in chloroform, and washed with methanol. The yield was 10%. TPP was then reacted with 1% solution of various metallic acetates in ethanol, and refluxed for 45 minutes to obtain respective metalloporphyrine but the better results were obtained with Ni-Acetate to give Ni-tetraphenylporphyrine, and its yield was found to be 87%.

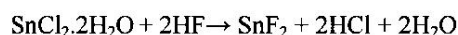
Preparation of SnO₂ Film

The film of SnO₂ was also made by a slight modification of the reported method [9] as described below.

Preparation of SnF₂ Solution

SnCl₂·2H₂O (99.5%), HF (40%), ethylenglycol (99.8%), and some other polar organic solvents like isopropanol, glycerol, and *n*-butanol were taken as starting materials. The equimolar solution of both HF, and SnCl₂·2H₂O was prepared separately. Tin chloride solution was prepared in organic (polar) solvent, and HF solution was prepared in water. Both the solutions were mixed in fixed atomic ratio of Sn:F (25:1 to 1:25) in separate 250 mL beakers. The resulting solutions were stirred, and refluxed for about an hour, and then allowed to stand for at least 24 hours for aging.

Chemical Reaction



Cleaning and Ultrasonication of Glass Substrate

Glass slides were first cut into suitable size with diamond cutter, washed with detergent, and tap water, distilled water, acetone, with distilled water, and at last with acetone in a sequential manner. After washing, the slides were dipped in a beaker containing 250 mL of acetone or ethanol. Then the beaker was placed in a sonicator, for at least 50 minutes to remove all types of adsorbed particles from the glass substrate. The sonicated slides were stored in doubly distilled water.

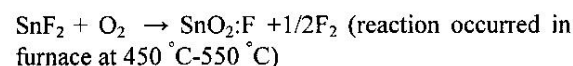
Dip-coating

SnF₂ (aged) solution was taken in the 250 mL beaker, and ultrasonically cleaned glass slides as substrates were first dipped into the solution, and then withdrawn vertically from the solution slowly at the rate of 6 cm/min for 20 to 25 times. Between two successive dipping the substrate along with the sol was dried at 80 °C–100 °C (depending upon the boiling point of solvent used) to have quick gelation. Thus the films got deposited layer by layer to achieve uniformity.

Annealing

After dip-coating slides were taken into the furnace, and heated up to 450 °C to 550 °C for oxidation of Sn. This temperature was maintained for about 15 to 20 minutes. The temperature was allowed to fall gradually to room temperature (it takes about 24 hours). In the furnace SnF₂ was converted (oxidized) into SnO₂:F. The possible reaction is given below.

Chemical Reaction:



Preparation of ZnO Solution

About 1% solution of ZnO was prepared in methanol, and refluxed for about 30 minutes to dissolve ZnO thoroughly in solvent or to get its homogenous colloidal solution.

Deposition of ZnO on Glass

ZnO solution was taken in 250 mL beaker, and glass slides deposited with SnO₂ : F were now dipped into this solution in a similar way as done before for the coating of SnF₂ solution. But before coating, one side of the slide was covered with tape, which was removed before drying. After dip-coating slides were again taken into the furnace, and annealed at 800 °C. Furnace was allowed to cool gradually until the room temperature was achieved [14].

Fabrication and Sealing

Glass electrode (anode) and platinized-aluminum-wrapped (cathode) electrode were taken. Few drops of dye solution were applied on glass electrode, allowed the dye to dry on the surface of the glass electrode. Few drops of electrolyte were also applied on the dye adsorbed glass electrode and then counter electrode was placed on it in such a way that it sandwiched the dye, and electrolyte. The sealing was done with the help of glue, and electrical connections were made [15].

Characterization

1. X-ray powder diffractometer (Xⁱ Pert PRO., PANalytical) with a monochromated CuK_α radiation ($\lambda = 1.540598 \text{ \AA}$) within a 2 θ range of 20-80° was employed to assess the crystallinity of the deposits at room temperature.
2. Surface morphology, and microstructure of the coating was investigated by SEM (JEOL-JSM-6480LV).
3. UV-Visible absorption spectra of the films were obtained with a Spectroscopic Ellipsometer M-2000 FITM J. A. Woollam Co., Inc.
4. Structure determination of dye by single crystal X-ray diffractometer (2001 Bruker-AXS)
5. Thickness of the film was calculated by surface profilometry, and thickness obtained about 100 nm.
6. The absorption spectra of Ni-tetraphenylporphrine were obtained with UV-2300 (Techcomp) spectrophotometer.

Conclusions

We have fabricated a dye-sensitized solar cell based on SnO₂ electrode sensitized by high molar extinction coefficient sensitizer (Ni-TPP). The SnO₂ electrode was successfully synthesized by Dip-coating. The effect of solvent on coating was studied, and concluded that volatility affected the deposition of film of glass substrate. The film was characterized by X-ray powder diffraction (XRD), SEM, and Ellipsometric analysis while the dye was analyzed by single crystal X-ray diffraction, and UV-Visible absorption spectroscopy. The band gap of the SnO₂ film has been estimated to be 3.8 eV. XRD shows that the formed SnO₂ has a tetragonal rutile crystal structure with crystalline size 2-5 nm. Thus the obtained nanocrystalline SnO₂ can be applied to dye-sensitized solar cell. The prepared cell was stable, and the degradation of dye was negligible under sunlight. It exhibited 2% photoelectric conversion. The fill factor calculated was 0.37, and V_{oc} = 0.60 All these results revealed the much better stability, and efficiency of our dye-sensitized solar cell.

References

1. D. Kuang, C. Klein, S. Ito, J-E. Moser, R. Humphry-Baker, N. Evans, F. Durrant, C. Grätzel, S. M. Zakeeruddin, and M. Grätzel, *Advanced Materials*, **19**, 1133 (2007).
2. P. Thangadurai, A. C. Bose, S. Ramasamy, R. Kesavamoorthy, and T. R. Ravindran, *Journal of Physics, and Chemistry of Solids*, **66**, 1621 (2005).
3. J. A. T. Antonio, R. G. Baez, P. J. Sebastian, and A. Vázquez, *Journal of Solid State Chemistry*, **174**, 241 (2003).
4. F. Legendre, S. Poissonnet, and P. Bonnailie, *Journal of Alloys and Compounds*, **434**, 400 (2007).
5. F. Gu, S. F. Wang, M. K. Lü, X. F. Cheng, S. W. Liu, G. J. Zhou, D. Xu, and D. R. Yuan, *Journal of Crystal Growth*, **262**, 182 (2004).
6. H. W. Kim, and S. H. Shim, *Journal of Alloys and Compounds*, **426**, 286 (2006).
7. T. Stergiopoulos, I. M. Arabatzis, H. Cachet, and P. Falaras, *Journal of Photochemistry, and Photobiology A: Chemistry*, **155**, 163 (2003).
8. H. Tian, P. H. Liu, W. Zhu, E. Gao, D. J. Wu, and S. Cai, *Journal of Material Chemistry*, **10**,

- 2708 (2000).
9. A. N. Banerjee, S. Kundoo, P. Saha, and K. K. Chattopadhyay, *Journal of Sol-Gel Science and Technology*, **28**, 105 (2003).
 10. Q. Wang, W. M. Campbell, E.E. Bonfantini, K. W. Jolley, D. L. Officer, P. J. Walsh, K. Gordon,
 11. R. Humphrey-Baker, M. K. Nazeeruddin and M. Grätzel, *Journal of Physical Chemistry B*, **109**, 15397 (2005).
 12. M. J. Hamor, T. A. Hamor, and J. L. Hoard, *Journal of American Chemical Society*, **86**, 1938 (1964).
 - Z. S. Wang, Y. Cui, K. Hara, Y. Dan-Ch, C. Kasada, and A. Shinpo, *Advanced Material*, **19**, 1138 (2007).
 13. A. D. Adler, F. R. Longo, J. D. Finarelli, J. Goldmacher, J. Assour, and L. Korsakoff, *Journal of Organic Chemistry*, **32**, 476 (1967).
 14. R. Singhal, M. S. Tomar, J. G. Burgos, A. Kumar, and R. S. Katiyar, *Materials Research Society, Symposium Proceedings*, **0972**, AA 06-07 (2006).
 15. D. Zhang, T. Yoshida, T. Oekermann, K. Furuta, and H. Minoura, *Advanced Functional Materials*, **16**, 1228 (2006).